Bayesian Framework to Wavelet Estimation and Linearized Acoustic Inversion

Leandro Passos de Figueiredo, Marcio Santos, Mauro Roisenberg, Guenther Schwedersky Neto, and Wagner Figueiredo

***Abstract*—In this letter, we show how a seismic inversion method based on a Bayesian framework can be applied on poststack seismic data to estimate the wavelet, the seismic noise level, and the subsurface acoustic impedance. We propose a different linearized forward model and discuss in detail how some stochastic quantities are defined in a geophysical interpretation. The forward model and the Gaussian assumption for the likelihood distributions enable to obtain the conditional distributions. The method is divided into two sequential steps: the wavelet and noise level estimation, in which the posterior distribution is obtained via the Gibbs sampling algorithm, and the acoustic inversion, which uses the proposal forward model and the results of the first step. In the second step, the posterior distribution for acoustic impedance is analytically obtained. Therefore, the maximum *a posteriori* impedance can be calculated, yielding a very fast inversion algorithm. Results of tests on real data are compared with the deterministic constrained sparse-spike inversion, indicating that our proposal is viable and reliable.**

***Index Terms*—Acoustic inversion, Bayesian framework, maximum *a posteriori* (MAP), reservoir characterization, seismic inversion, wavelet estimation.**

I. Introduction

SEISMIC inversion is an important tool widely used in geophysical problems [1], [2] to infer the subsurface properties through seismic wave measurements. In particular, it can improve exploration and management success in the petroleum industry since it estimates the elastic properties from the seismic data, which has a great correlation with many petrophysical properties. The major challenge of the seismic inversion method is to integrate all different kinds of data in order to obtain an accurate and high resolution set of subsurface parameters, also characterizing the uncertainties of the results of the inversion.

In general, the techniques proposed to solve the seismic inversion problem, such as simulated annealing, genetic algorithms, particle swarm optimization, etc., are based on optimization procedures [3]–[5] and are strongly dependent on computational resources. However, more recently, a stochastic Bayesian formulation for the inverse problem has been proposed and used as an efficient and robust technique to estimate not only one solution of the subsurface properties but also an ensemble of high accuracy solutions, which allows an estimate of the uncertainties associated with these properties [1], [6]–[8].

The stochastic Bayesian formulation for the seismic inversion involves the determination of the posterior distribution using a sampling algorithm. In this letter, we have used the Gibbs algorithm that is a Markov chain Monte Carlo (MCMC) method, similar to the Metropolis one, in order to perform multiple samplings of the posterior distribution through a random walk in the parameter space [9], [10]. Then, based on [11], we develop a stochastic Bayesian algorithm for wavelet and noise level estimation, and we explicitly show how some quantities of our model are defined in a geophysical interpretation. Moreover, we adapt the Bayesian elastic inversion method proposed in [12] and [7] for the linearized acoustic inversion of poststack seismic data. In contrast with previous works that directly use the equations of the convolutional model [3], [13], we use a different approach, in which the model vector is a logarithm function of the impedance and the forward operator involves a differential matrix [14]. This procedure simplifies the determination of the posterior distribution.

The stochastic wavelet estimation results and the Gaussian assumption for the likelihood distributions enable us to obtain the analytical form of the posterior distribution of the acoustic impedance. The maximum *a posteriori* (MAP) solution for the inverse problem can also be determined with a low computational cost.

II. Methodology

A. Seismic Model

Assuming that the seismic data were processed to remove the multiple reflections and other undesirable effects, the forward seismic model can be considered as the convolutional model

$$d_o(t) = \int_{-\infty}^{\infty} s(\tau) r(t-\tau) d\tau + e_d(t) \tag{1}$$

where $d_o(t)$ is a seismic trace, $s(t)$ is the wavelet, $e_d(t)$ is a random noise, and $r(t)$ is the weak contrast reflectivity that depends on acoustic impedance $z(t)$ by the following relation:

$$r(t) = \frac{1}{2} \partial \ln (z(t)) . \tag{2}$$

Equation (1), in a discrete version [15], can be rewritten as

$$\boldsymbol{d}_o = \boldsymbol{R}\boldsymbol{s} + \boldsymbol{e}_d \tag{3}$$

Manuscript received May 23, 2013; revised October 11, 2013 and January 27, 2014; accepted April 27, 2014. Date of publication May 20, 2014; date of current version June 20, 2014.

L. Passos de Figueiredo, M. Santos, M. Roisenberg, and W. Figueiredo are with the Federal University of Santa Catarina, 88040-900 Florianopolis-SC, Brazil (e-mail: leandrop.fgr@gmail.com).

G. S. Neto is with the Petrobras, 20031-912 Rio de Janeiro, Brazil.

Color versions of one or more of the figures in this paper are available online at http://ieeexplore.ieee.org.

Digital Object Identifier 10.1109/LGRS.2014.2321516

or

$$\boldsymbol{d}_o = \boldsymbol{S}\boldsymbol{r} + \boldsymbol{e}_d \tag{4}$$

where the vectors are the discrete representations of the variables of (1), $\boldsymbol{S}$ is the convolutional matrix formed by the wavelet $\boldsymbol{s}$, and $\boldsymbol{R}$ is the convolutional matrix formed by the reflectivity $\boldsymbol{r}$.

When reflectivity is defined by (2), some mathematical difficulties arise as can be seen in [7]. To avoid that, a differential operator $\boldsymbol{D}$ is used instead. In fact, defining a linear operator $\boldsymbol{G} = (1/2)\boldsymbol{S}\boldsymbol{D}$ and a model vector $\boldsymbol{m} = \ln(\boldsymbol{z})$, a simple linear relation between the seismic data and the model parameters can be obtained

$$\boldsymbol{d}_o = \boldsymbol{G}\boldsymbol{m} + \boldsymbol{e}_d. \tag{5}$$

B. Stochastic Model

In our stochastic model, the distributions are considered multivariate normal distributions. They are denoted by $N_n(\boldsymbol{\mu}, \boldsymbol{\Sigma})$, where $\boldsymbol{\mu}$ is the mean vector, $\boldsymbol{\Sigma}$ is the covariance matrix, and n is the dimension of $\boldsymbol{\mu}$ and $\boldsymbol{\Sigma}$. Their explicit form is expressed by

$$p(\boldsymbol{x}) = \frac{1}{(2\pi)^{\frac{n}{2}} |\boldsymbol{\Sigma}|^{\frac{1}{2}}} \exp\left(-\frac{1}{2}(\boldsymbol{x}-\boldsymbol{\mu})^T \boldsymbol{\Sigma}^{-1}(\boldsymbol{x}-\boldsymbol{\mu})\right) \tag{6}$$

where $\boldsymbol{x}$ is a random field that satisfies the multivariate distribution [16].

Assuming that seismic noise $\boldsymbol{e}_d$ is Gaussian and based in (3) and (5), we propose a likelihood distribution for $\boldsymbol{d}_o$, with expectation value $\boldsymbol{\mu}_d = \boldsymbol{R}\boldsymbol{s}$ (3) or $\boldsymbol{\mu}_d = \boldsymbol{G}\boldsymbol{m}$ (5) and covariance matrix $\boldsymbol{\Sigma}_d$ as

$$p(\boldsymbol{d}_o|\boldsymbol{\mu}_d, \boldsymbol{\Sigma}_d) = N_{n_d}(\boldsymbol{\mu}_d, \boldsymbol{\Sigma}_d). \tag{7}$$

The likelihood distribution for the wavelet is also a Gaussian distribution. It is given by

$$p(\boldsymbol{s}|\boldsymbol{\mu}_s, \boldsymbol{\Sigma}_s) = N_{n_s}(\boldsymbol{\mu}_s, \boldsymbol{\Sigma}_s) \tag{8}$$

where the wavelet expectation value $\boldsymbol{\mu}_s$ is defined by a null vector with n_s components.

For the model vector $\boldsymbol{m}$, we define the following normal likelihood distribution:

$$p(\boldsymbol{m}|\boldsymbol{\mu}_m, \boldsymbol{\Sigma}_m) = N_{n_m}(\boldsymbol{\mu}_m, \boldsymbol{\Sigma}_m) \tag{9}$$

where the covariance matrix $\boldsymbol{\Sigma}_m$ is related to the temporal correlation between the components of $\boldsymbol{m}$ and will be defined later. The expectation $\boldsymbol{\mu}_m$ is defined by the natural logarithm of the low frequency impedance model, which is obtained through the interpolation of well data [17].

The covariance matrices are assumed to be known up to an unknown multiplicative variance factor σ_v^2

$$\boldsymbol{\Sigma}_v = \sigma_v^2 \boldsymbol{\Sigma}_{0v} \qquad \forall \boldsymbol{v} \in \{\boldsymbol{m}, \boldsymbol{s}, \boldsymbol{d}\} \tag{10}$$

where the covariance matrix structures $\boldsymbol{\Sigma}_{0v}$ are defined using the prior knowledge about the quantities of interest. For instance, for the wavelet, we know that its components approach to zero at the ends, while for the model vector, we use the fact that its components have correlation with its neighbors.

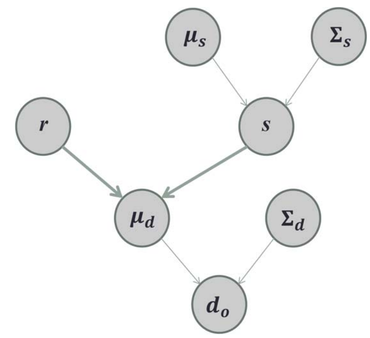

Fig. 1. DAG representing the stochastic model for wavelet and noise level estimation.

C. Stochastic Wavelet Estimation

To estimate the wavelet, the method is applied in the well location, where the reflectivity $\boldsymbol{r}$ can be directly calculated. The quantities and their relations, defined in (3), and the likelihood distributions of (7) and (8) can be represented in a directed acyclic graph (DAG), which is a useful tool very used in graph theory [18]. Here, a DAG (see Fig. 1) is used in order to obtain an expression for the posterior distribution [11], [19].

To complete our stochastic model, we consider the prior distributions for the unknown variance factors σ_d^2 and σ_s^2 as uniform distributions. On the other hand, the expectation $\boldsymbol{\mu}_s$ and the reflectivity $\boldsymbol{r}$ are considered to be completely known, and their prior distributions are delta distributed.

The components of the wavelet covariance matrix $\boldsymbol{\Sigma}_{0s}$, which correspond to the covariance between the wavelet elements s_t and $s_{t'}$ at the times t and t', are defined by

$$\boldsymbol{\Sigma}_{0s_{t,t'}} = \delta_t \delta_{t'} \exp\left(-\frac{(t-t')^2}{L_s^2}\right) \tag{11}$$

where

$$\delta_t = \exp\left(-\frac{1}{0.02 n_s^2}(t-(n_s+1)/2)^2\right). \tag{12}$$

The parameter L_s is defined by observing the range of the seismic vertical variogram, which is assumed to be approximately equal to the wavelet variogram range. The exponential term in (11) is a correlation function that imposes smoothness for the wavelet, while the variance of the wavelet components δ_t ensures that the wavelet components approach zero at the ends.

We have also considered $\boldsymbol{e}_d$ as a white noise and the covariance matrix for the seismic data $\boldsymbol{\Sigma}_{0d}$ as a simple identity matrix.

From the joint distribution related to the DAG of Fig. 1, the posterior distribution can be obtained, without the normalization factor [19], by

$$p\left(\boldsymbol{s}, \sigma_s^2, \sigma_d^2 | \boldsymbol{d}_o, \boldsymbol{r}, \boldsymbol{\mu}_s\right) \propto p\left(\boldsymbol{d}_o | \boldsymbol{s}, \boldsymbol{r}, \sigma_d^2\right) p\left(\boldsymbol{s} | \boldsymbol{\mu}_s, \sigma_s^2\right). \tag{13}$$

Unfortunately, it is not easy to find an analytical expression for this probability. Due to this fact, an MCMC algorithm is necessary. More specifically, the Gibbs algorithm is used for sampling from the posterior distribution. For each interaction, we draw the unknown quantities, given all the others, and calculate the mean value and the uncertainties of the variables of interest.

1) Algorithm: In order to develop the Gibbs algorithm, we need the conditional distributions for the unknown quantities [9], [10]. The conditional distribution for the wavelet is obtained using (13), considering a given set of fixed quantities together with the seismic model of Section II-A. Moreover, we need to use the theorem of the conditional distribution of multivariate Gaussian distributions and also the distribution of a nonsingular linear transformation theorem, which can be found in [16]. Then, after some algebraic manipulations, the conditional distribution for $\boldsymbol{s}$ is

$$p\left(\boldsymbol{s}|\boldsymbol{\mu}_s, \boldsymbol{d}_o, \boldsymbol{m}, \sigma_d^2, \sigma_s^2\right) = N(\boldsymbol{\mu}_{s|}, \boldsymbol{\Sigma}_{s|}) \tag{14}$$

where the expectation value and the covariance matrix are

$$\boldsymbol{\mu}_{s|} = \boldsymbol{\mu}_s + \boldsymbol{\Sigma}_s \boldsymbol{R}^T \left(\boldsymbol{R}\boldsymbol{\Sigma}_s\boldsymbol{R}^T + \boldsymbol{\Sigma}_d\right)^{-1} (\boldsymbol{d}_o - \boldsymbol{R}\boldsymbol{\mu}_s) \tag{15}$$

$$\boldsymbol{\Sigma}_{s|} = \boldsymbol{\Sigma}_s - \boldsymbol{\Sigma}_s \boldsymbol{R}^T \left(\boldsymbol{R}\boldsymbol{\Sigma}_s\boldsymbol{R}^T + \boldsymbol{\Sigma}_d\right)^{-1} \boldsymbol{R}\boldsymbol{\Sigma}_s. \tag{16}$$

On the other hand, the conditional distribution for the multiplicative variance factor σ_v^2 (for all $\boldsymbol{v} \in \{\boldsymbol{s}, \boldsymbol{d}\}$) is derived using (13) and considering the other parameters as constants. In this case, we can show that this distribution is the inverse-gamma [10]

$$\sigma_v^2 \sim IG(\gamma_v, \lambda_v) \tag{17}$$

in which the shape γ_v and the scale λ_v parameters are given by

$$\gamma_v = \frac{n_v}{2}, \quad \lambda_v = \frac{(\boldsymbol{v} - \boldsymbol{\mu}_v)^T \boldsymbol{\Sigma}_{0v}^{-1} (\boldsymbol{v} - \boldsymbol{\mu}_v)}{2}. \tag{18}$$

The Gibbs algorithm is summarized hereinafter.

Algorithm 1 Algorithm for the stochastic wavelet estimation

```
Define initial values for σ_d^2 and σ_s^2
for i = 1, ..., k + n do
    Draw s(i) from (14)–(16)
    Draw σ_v^2(i) from (17) and (18)
    Σ_v = σ_v^2(i) Σ_0v ∀ v ∈ {s, d}
end for
```

Here, k is the number of iterations (samples) for the three quantities attaining a stationary condition, in which they are independent of k and therefore begin to fluctuate around its mean values. The mean values are calculated using n samples. In general, we used $k = 500$ and $n = 500$.

D. Acoustic Inversion

Based on the convolutional model (5) and the likelihood distributions (7) and (9), a stochastic model for the acoustic inversion is proposed in the DAG shown in Fig. 2.

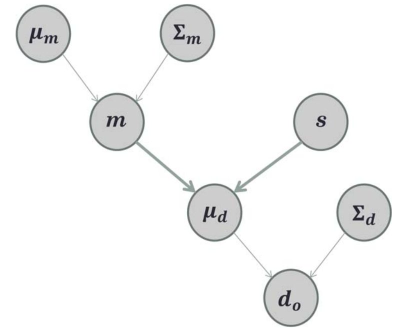

Fig. 2. DAG representing the stochastic model for acoustic inversion.

The covariance matrix components of the model vector $\boldsymbol{m}$ are defined by

$$\Sigma_{0m_{t,t'}} = \exp\left(-\frac{(t-t')^2}{L_t^2}\right) \tag{19}$$

where the temporal range parameter L_t is related to the vertical resolution of the acoustic impedance. Therefore, it is adjusted at hand to be smaller than the seismic variogram range, in order to increase the impedance resolution compared to the seismic one.

To determine the posterior distribution for the vector model $\boldsymbol{m}$, we take into account the wavelet $\boldsymbol{s}$ and σ_d^2 obtained by the stochastic wavelet estimation presented in Section II-C [12]. Moreover, we have considered the model expectation $\boldsymbol{\mu}_m$ as the logarithm of the impedance low frequency model and σ_m^2 as the variance of the well impedance logarithm around $\boldsymbol{\mu}_m$. In this case, the associated prior distributions are delta ones, simplifying the posterior distribution, which is given by

$$p\left(\boldsymbol{m}|\boldsymbol{d}_o, \boldsymbol{s}, \boldsymbol{\mu}_m, \sigma_d^2, \sigma_m^2\right) \propto p\left(\boldsymbol{d}_o|\boldsymbol{s}, \boldsymbol{m}, \sigma_d^2\right) p\left(\boldsymbol{m}|\boldsymbol{\mu}_m, \sigma_m^2\right). \tag{20}$$

Now, using the same procedure and theorems employed to calculate the wavelet conditional distribution, mentioned in Section II-C, the posterior distribution is obtained analytically and is given by

$$p\left(\boldsymbol{m}|\boldsymbol{d}_o, \boldsymbol{s}, \boldsymbol{\mu}_m, \sigma_d^2, \sigma_m^2\right) = N(\boldsymbol{\mu}_{m|}, \boldsymbol{\Sigma}_{m|}) \tag{21}$$

where the expectation value $\boldsymbol{\mu}_{m|}$ and the covariance matrix $\boldsymbol{\Sigma}_{m|}$ are

$$\boldsymbol{\mu}_{m|} = \boldsymbol{\mu}_m + \boldsymbol{\Sigma}_m \boldsymbol{G}^T \left(\boldsymbol{G}\boldsymbol{\Sigma}_m\boldsymbol{G}^T + \boldsymbol{\Sigma}_d\right)^{-1} (\boldsymbol{d}_o - \boldsymbol{G}\boldsymbol{\mu}_m) \tag{22}$$

$$\boldsymbol{\Sigma}_{m|} = \boldsymbol{\Sigma}_m - \boldsymbol{\Sigma}_m \boldsymbol{G}^T (\boldsymbol{G}\boldsymbol{\Sigma}_m\boldsymbol{G}^T + \boldsymbol{\Sigma}_d)^{-1} \boldsymbol{G}\boldsymbol{\Sigma}_m. \tag{23}$$

As the posterior is a multivariate normal distribution, the MAP solution is the posterior expectation $\boldsymbol{\mu}_{m|}$.

To resume, the developed methodology for a fast MAP algorithm to the acoustic inversion of poststack seismic data consists in applying the stochastic wavelet estimation, and after that, use its results to define the quantities involved in the stochastic model of Fig. 2. Finally, calculating the exponential of (22), we can obtain the MAP acoustic impedance for each seismic trace.

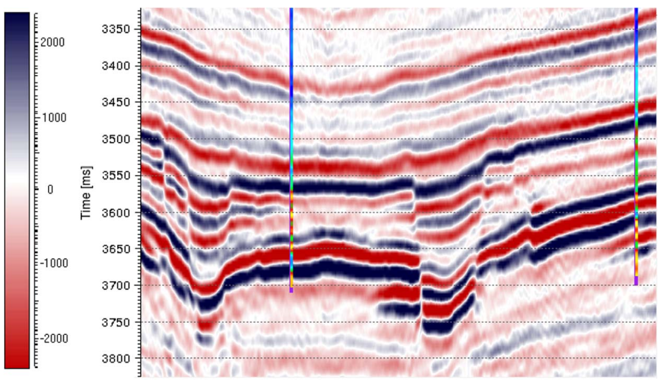

Fig. 3. Arbitrary line of the poststack seismic cube applied to the inversion method with the well data.

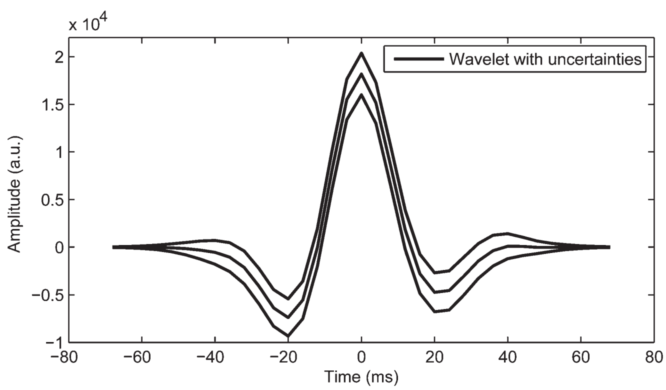

Fig. 4. Estimated wavelet in arbitrary units and its uncertainty.

Other interesting application is the use of the posterior covariance to perform the stochastic sampling of impedance, obtaining high resolution realizations of the subsurface [8].

III. Experiments and Results

To evaluate the algorithm efficiency, the method presented in Section II is applied on real poststack seismic data. The studied area consists of a cube with 1 s in two-way travel-time thickness, 500 inlines, and 345 crosslines, using 4 ms and 25 m for the sampling interval. The results are shown only for a small part of the entire cube (see Fig. 3).

In this application, the range parameter L_s of the wavelet correlation function of (11) is considered to be 10 ms, while for the covariance matrix in (19), the range parameter L_t is 6 ms. Based on the Gibbs algorithm of the stochastic wavelet estimation, the results are calculated after 30 iterations to ensure the convergence to the posterior distribution in (13). The mean wavelet calculated with the uncertainty for each point is shown in Fig. 4, while the histogram of the seismic noise variance σ_d^2, sampled during the same algorithm, is shown in Fig. 5. This figure illustrates the posterior distribution of σ_d^2.

As described in Section II-D, using these results, the well data, and the low frequency model, shown in Fig. 6, the full band MAP solution is obtained through (22). It is shown in Fig. 7. This same result is also shown in the limited band range from 8 to 60 Hz in Fig. 8.

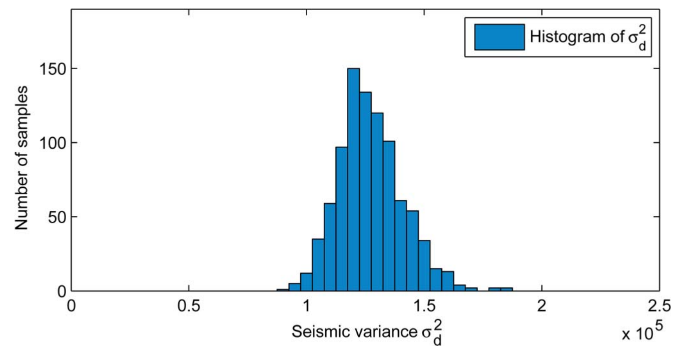

Fig. 5. Histogram of seismic noise variance σ_d^2 sampled during the algorithm.

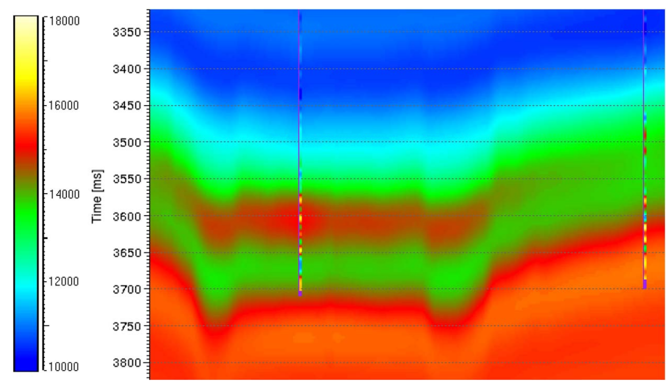

Fig. 6. Low frequency model used to define the model expectation values $\boldsymbol{\mu_m}$ with the well data.

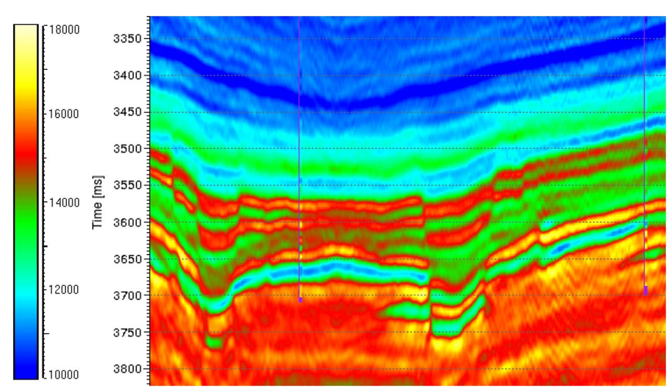

Fig. 7. Map solution of the acoustic impedance with the well data.

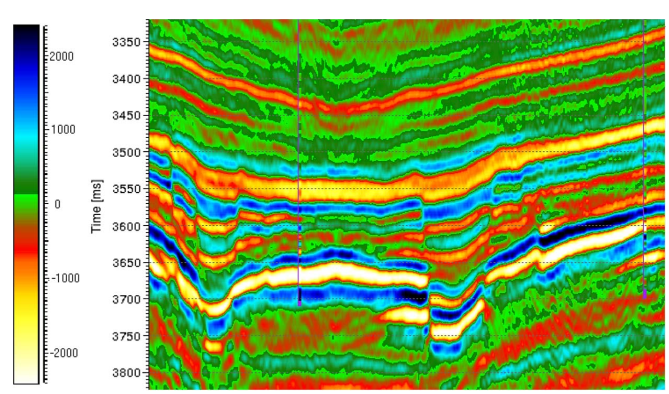

Fig. 8. Map solution of the acoustic impedance with the well data, both in the limited band from 8 to 60 Hz.

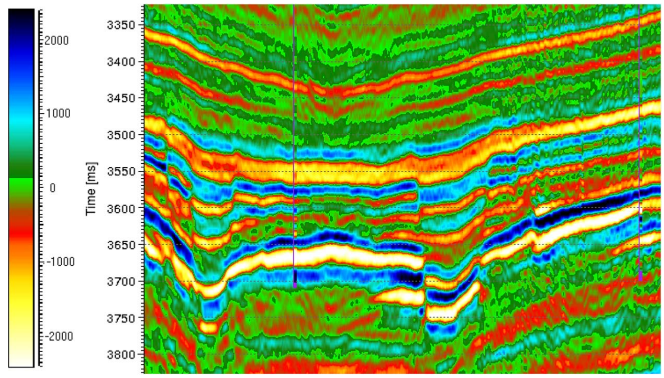

Fig. 9. Deterministic inversion obtained from constrained sparse-spike method with the well data, both in limited band from 8 to 60 Hz.

TABLE I
CORRELATION BETWEEN THE WELL DATA AND THE INVERSION METHODS (BOTH IN LIMITED BAND FROM 8 TO 60 Hz)

Inversion	Well1	Well2	Well3	Well4
Bayesian Inversion	0.72	0.87	0.85	0.91
CSSI	0.68	0.88	0.83	0.91

To analyze the inversion quality, we compare our MAP solution with the inversion in Fig. 9, obtained by the constrained sparse-spike inversion (CSSI) method [5]. As we can see, they appear very similar when we use the same wavelet and the same limited band. However, the Bayesian inversion is faster than the sparse-spike method. In fact, while the calculation of the MAP solution takes 5 min, the sparse-spike optimization takes 30 min to invert the same seismic cube.

For all the inversion results, the well acoustic impedance data are shown in the same color scale. As we can see, our results are in agreement with the well data, showing that the inversion procedure is of high quality. Moreover, to quantify the quality of the inversion, we have calculated the correlation between the well data and the inversion, with both of them in limited band range from 8 to 60 Hz, as shown in Table I.

As can be seen, our Bayesian inversion exhibits a good correlation with the well data, which is very similar to the sparse-spike inversion, but with less computational cost.

IV. CONCLUSION

We have introduced a methodology to the fast MAP algorithm for the acoustic inversion of poststack seismic data. In the wavelet estimation, the method presents good results without any assumption about the wavelet phase. The estimated wavelet and the mean value of the noise level yield good results when used as fixed quantities in the proposed acoustic inversion method. The methodology appears to be a good choice for acoustic inversion, due to the possibility of integrating prior knowledge, such as the low frequency model, seismic variogram, and wavelet characteristics, in the inversion results conditioned to seismic traces. The similarity between the MAP solution and the CSSI indicates the feasibility and reliability of the proposed method. The covariance matrix calculations of the multivariate Gaussian distributions are important procedures to incorporate the results of the prior knowledge into the inversion, which directly influences its quality.

ACKNOWLEDGMENT

The authors would like to thank Fugro-Jason for providing the academic licensed software for this research and also Conselho Nacional de Pesquisa e Desenvolvimento, Fundação de Amparo à Pesquisa e Inovação do Estado de Santa Catarina, and Petrobras for their support and availability during the work.

REFERENCES

[1] M. Bosch, T. Mukerji, and E. F. Gonzalez, “Seismic inversion for reservoir properties combining statistical rock physics and geostatistics: A review,” *Geophysics*, vol. 75, no. 5, pp. 75A165–75A176, 2010.

[2] K. Aki and P. G. Richards, *Quantitative Seismology*. Mill Valley, CA, USA: University Science Books, 2002.

[3] C. R. Conti, M. Roisenberg, G. Neto, and M. J. Porsani, “Fast seismic inversion methods using ant colony optimization algorithm,” *IEEE Geosci. Remote Sens. Lett.*, vol. 10, no. 5, pp. 1119–1123, Sep. 2013.

[4] S. Oliveira, L. Loures, F. Moraes, and C. Theodoro, “Nonlinear impedance inversion for attenuating media,” *Geophysics*, vol. 74, no. 6, Nov. 2009.

[5] R. B. Latimer and P. Riel, “Integrated seismic reservoir characterization and modeling: A Gulf of Mexico 3D case history,” presented at the GCSSEPM Res. Conf., 1996, pp. 1–10.

[6] K. Rimstad, P. Avseth, and H. Omre, “Hierarchical Bayesian lithology/fluid prediction: A North Sea case study,” *Geophysics*, vol. 77, no. 2, pp. B69–B85, 2012.

[7] A. Buland and H. Omre, “Joint AVO inversion, wavelet estimation and noise-level estimation using a spatially coupled hierarchical Bayesian model,” *Geophys. Prosp.*, vol. 51, no. 6, pp. 531–550, 2003.

[8] A. Buland, O. Kolbjørnsen, and H. Omre, “Rapid spatially coupled AVO inversion in the Fourier domain,” *Geophysics*, vol. 68, no. 3, pp. 824–836, 2003.

[9] S. Geman and D. Geman, “Stochastic relaxation, Gibbs distributions, and the Bayesian restoration of images,” *IEEE Trans. Pattern Anal. Machine Intell.*, vol. PAMI-6, no. 6, pp. 721–741, 1984.

[10] A. Gelman, J. B. Carlin, H. S. Stern, and D. B. Rubin, *Bayesian Data Analysis*. London, U.K.: Chapman & Hall, 2004.

[11] A. Buland and H. Omre, “Bayesian wavelet estimation from seismic and well data,” *Geophysics*, vol. 68, no. 6, pp. 2000–2009, 2003.

[12] A. Buland and H. Omre, “Bayesian linearized AVO inversion,” *Geophysics*, vol. 68, no. 1, pp. 185–198, 2003.

[13] J. Gunning and M. E. Glinsky, “Delivery: An open-source model-based Bayesian seismic inversion program,” *Comput. Geosci.*, vol. 30, no. 6, pp. 619–636, Jul. 2004.

[14] E. L. Bongajum, J. Boisvert, and M. D. Sacchi, “Bayesian linearized seismic inversion with locally varying spatial anisotropy,” *J. Appl. Geophysics*, vol. 88, pp. 31–41, Jan. 2013.

[15] M. K. Sen, *Seismic Inversion*. Richardson, TX, USA: Soc. Petroleum Eng., 2006.

[16] T. W. Anderson, *An Introduction to Multivariate Statistical Analysis*. Hoboken, NJ, USA: Wiley, 1984, ser. Wiley Series in Probability and Mathematical Statistics: Probability and Mathematical Statistics.

[17] T. M. Hansen, K. Mosegaard, R. Pedersen-tatalovic, A. Uldall, and N. L. Jacobsen, “Attribute-guided well-log interpolation applied to low-frequency impedance estimation,” *Geophysics*, vol. 73, no. 6, pp. R83–R95, 2008.

[18] R. J. Trudeau, *Introduction to Graph Theory*. New York, NY, USA: Dover, 1993, ser. Dover Books on Advanced Mathematics.

[19] W. R. Gilks, S. Richardson, and D. J. Spiegelhalter, *Markov Chain Monte Carlo in Practice*. London, U.K.: Chapman & Hall, 1996, ser. Interdisciplinary Statistics.